Available online at www.sciencedirect.com
SCIENCE DIRECT®
Composites Science and Technology 65 (2005) 693–702
COMPOSITES SCIENCE AND TECHNOLOGY
www.elsevier.com/locate/compscitech

Strength distribution of elementary flax fibres

J. Andersons [a,*], E. Spārniņš [a], R. Joffe [b], L. Wallström [b]

[a] Institute of Polymer Mechanics, University of Latvia, Aizkraukles iela 23, Rīga LV-1006, Latvia
[b] Division of Polymer Engineering, Luleå University of Technology, SE-971 87 Luleå, Sweden

Received 15 April 2004; received in revised form 21 September 2004; accepted 4 October 2004
Available online 11 November 2004

Abstract

Flax fibres, along with a number of other natural fibres, are being considered as an environmentally friendly alternative of synthetic fibres in fibre-reinforced polymer composites. A common feature of natural fibres is a much higher variability of mechanical properties. This necessitates study of the flax fibre strength distribution and efficient experimental methods for its determination. Elementary flax fibres of different gauge lengths are tested by single fibre tension in order to obtain the stress–strain response and strength and failure strain distributions. The applicability of single fibre fragmentation test for flax fibre failure strain and strength characterization is considered. It is shown that fibre fragmentation test can be used to determine the fibre length effect on mean fibre strength and limit strain.

Keywords: A. Fibres; B. Fragmentation; B. Mechanical properties; C. Statistics; Flax

1. Introduction

Ecological concerns have resulted in a renewed interest in natural materials, and such issues as recyclability and environmental safety have become increasingly important for the introduction of new materials and products. Structural polymer composites are traditionally utilizing man-made fibres (such as glass or carbon fibres) as reinforcement, but environmental issues have generated a considerable interest in natural fibres. Plant fibres such as flax, hemp, sisal and kenaf are under consideration as environmentally friendly and relatively low-cost alternatives for glass fibres in structural engineering composites [1–3]. However, their use currently is mainly confined to reinforcement in compounded thermoplastic products similar to glass-mat-reinforced thermoplastics. These natural fibre mat thermoplastics are used in the automotive sector, in interior and exterior components [4,5].

Flax fibres used as reinforcement are located in the bast of the flax plant. The fibres are typically extracted by retting followed by mechanical processing (scutching and hackling). The mechanical properties of the obtained fibres are affected by the natural variability in plant and by the processing stage and damage sustained during processing [6–8] and thus have considerable scatter. Therefore, a simple and efficient method for fibre strength evaluation is needed. The mechanical tests of elementary flax fibres [6,8–10] revealed that fibre strength is reasonably well approximated by the two-parameter Weibull distribution. Single fibre fragmentation (SFF) test has been used as an efficient alternative to single fibre tensile (SFT) test for Weibull distribution parameter determination of synthetic fibres, while for flax fibres the test is mainly applied for the assessment of fibre/matrix adhesion [10–13]. The principal objective of the present study is to evaluate the applicability of

* Corresponding author. Tel.: +371 754 3327; fax: +371 782 0467.
E-mail address: janis.andersons@pmi.lv (J. Andersons).

0266-3538/$ - see front matter © 2004 Elsevier Ltd. All rights reserved.
doi:10.1016/j.compscitech.2004.10.001

SFF test for elementary flax fibre strength and limit strain characterization.

2. Experimental

2.1. Materials

Flax fibres delivered by FinFlax Oy (Finland) were used. The fibres had been enzyme retted for 22 h. The fibres were stored and tested at ambient conditions. The resins used in single fibre composite (SFC) specimens were vinyl ester (VE) and unsaturated polyester (UP).

2.2. Single fibre tensile tests

2.2.1. Specimen preparation

Single fibres were carefully manually separated from the bundles. Fibre ends were glued onto a paper frame according to the preparation procedure described in ASTM D 3379-75 Standard. During mounting the specimens were handled only by the paper frame. Fibre length outside the frame (gauge length) was 5, 10 or 20 mm. Upon clamping of the ends of the paper frame by the grips of the test machine, frame sides were carefully cut in the middle.

2.2.2. Test setup

The tests were carried out on an electromechanical tensile machine equipped with mechanical grips. Load–displacement curve was recorded during the test. Upper grip of the machine was attached through a hinge and thus allowed to self-align. All tests were displacement controlled with the loading rate of 0.5 mm/min.

Since the fibres were not pre-stretched before the test, there was an initial displacement before load was actually applied to the fibre. The amount of this displacement was defined as an interval from the beginning of the test until the point at which load increase is observed. It was discounted later on during data processing.

Although flax fibre cross-section has a polygonal shape (see Fig. 1) and fibre thickness varies somewhat along the fibre [14], we treated each fibre as perfectly round and having a constant diameter in order to simplify analysis. Fibre diameter was evaluated from optical observations under microscope as the average of five apparent diameter measurements taken at different locations along the fibre.

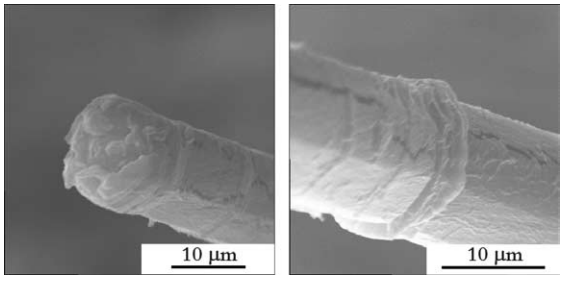

Fig. 1. Polygonal shape of the flax fibre.

2.3. Fibre fragmentation tests

2.3.1. Specimen preparation

Although single fibre fragmentation test is not strictly standardized, there are certain techniques that are established and widely used on synthetic fibres. The techniques may vary depending on particular experimental setup, but generally they include the following steps: single fibre separation from bundle, fibre pre-stretching (only to straighten the filament), mounting of the fibre on the frame and casting of the resin in the mould with the frame (see, e.g. [15]). Our experimental procedure applied for synthetic fibres [16,17] includes strain measurement by extensometer, therefore certain length of the samples is required. Hence specimen preparation procedure for the short fibres had to be modified in order to obtain specimens with length that would allow use of extensometer. The short flax fibres were modified by attaching fibre extensions on both ends of the filament, see Fig. 2. Thin fishing line of 90 μm diameter was used as fibre extensions. Once ''extended'' fibre is obtained it can be handled as any other long fibre. Further specimen preparation is according to the procedure described below (it also includes slight fibre pre-stretching in order to straighten the filament).

SFC specimens were prepared by mounting the extended fibres on a 1-mm thick steel frame, using double-sided adhesive tape. The frame was then placed between two flat Teflon-coated aluminium mould plates, separated by spacers of 2 mm thickness and provided with a silicon tube sealing. Mylar film was attached to the mould in order to obtain smooth and transparent surface. After the resin had solidified, the mould was placed in the oven for post-curing. VE was post-cured at 50 °C for 2 h and 80 °C for 5 h, UP was post-cured at 50 °C for 2 h. The plates were cut and polished into specimens with the dimensions shown in Fig. 3. Visual inspection revealed that the SFC specimens thus obtained were of uniform quality, with well-aligned fibres and no discernible bubbles or voids.

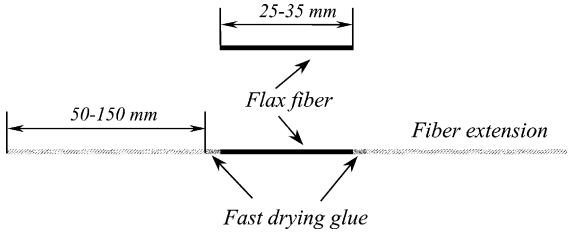

Fig. 2. Modification of flax fibre.

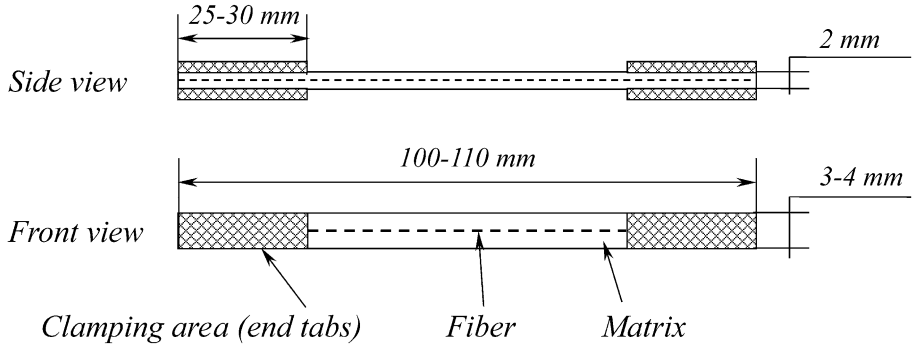

Fig. 3. SFC specimen.

The effect of fibre extensions on the stress state in a SFC and on SFF test results is discussed in Appendix A.

2.3.2. Test setup

The SFF test was performed in a MINIMAT miniature mechanical test machine from Polymer Laboratories Ltd (UK). The test machine was mounted on the *x–y* table of a Zeiss optical microscope. Load was measured by the MINIMAT's built-in load cell (1000 N) and the displacement was registered by the electronic unit of the tensile stage. Fragmentation of the fibres was observed during the loading. Extensometer was used to measure applied strain. In order to avoid pausing the machine to count fibre cracks, the test was carried out at rather low loading rate of 0.1 mm/min. Loading was stopped if the specimen failed, or when the fragmentation saturation level was achieved, namely, no new fibre breaks appeared with strain increase by 0.5%. During the experiment the data were transferred to the PC.

In order to measure the fibre diameter, digital pictures of the fibres were made before the loading. Images were made by the CCD camera attached to the microscope and then transferred to the PC for further processing. As in the case of single fibre tests fibre diameter was evaluated from analysis of digital images as the average of five apparent diameter measurements taken along the fibre.

3. Single fibre tensile test results

3.1. Stress–strain response

Not only limit stress and strain, but also the actual shape of the stress–strain curve was found to vary among fibres, ranging from linear elastic to markedly strain-hardening. (Note that similar variability in mechanical response was also observed for hemp fibres [18]). A typical stress–strain diagram of an elementary flax fibre is shown in Fig. 4. The apparent variation of

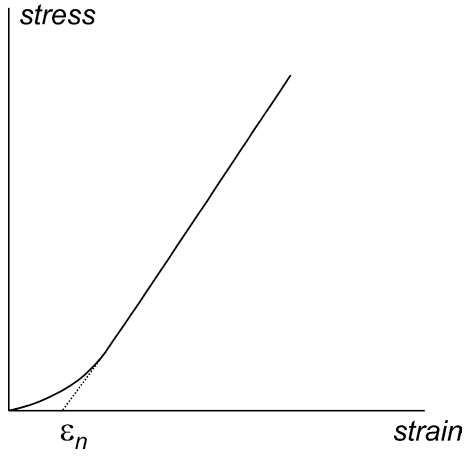

Fig. 4. Typical stress–strain curve of flax fibre.

tangent modulus with strain confined mostly to the initial, small strain part of the diagram (reported for flax fibres in e.g. [14,19]) is attributed to the orientation of the fibrils along the axis of the fibre under load. (This phenomenon is irreversible in that upon unloading, subsequent reloading is linear elastic up to the previously achieved stress level with the modulus equal to the maximum modulus achieved during the previous load cycle [14].) At larger load/strain values, fibre response becomes linear, and we use the linear part of diagram for Young's modulus calculation. There is a marked scatter of the measured modulus, E, values as seen in Fig. 5. The probabilities here and in the following are estimated as median ranks assigned to the measured modulus values at each gauge length using the following approximation:

$$P = \frac{i - 0.3}{m + 0.4},$$

where i is the ith number in ascendingly ordered modulus data and m is the sample size (i.e., number of modulus measurements performed at the given gauge length). The average value and standard deviation of

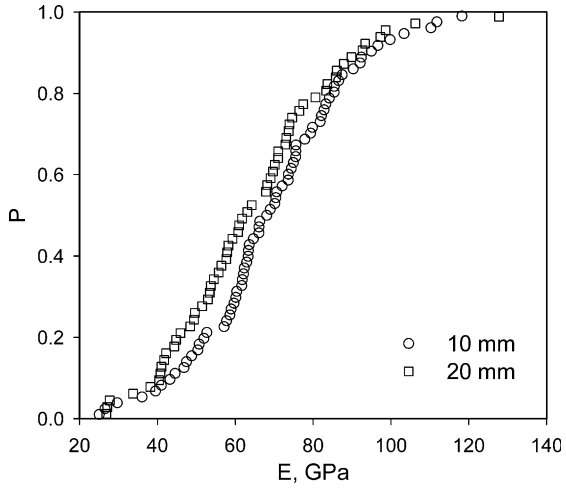

Fig. 5. Young's modulus distribution.

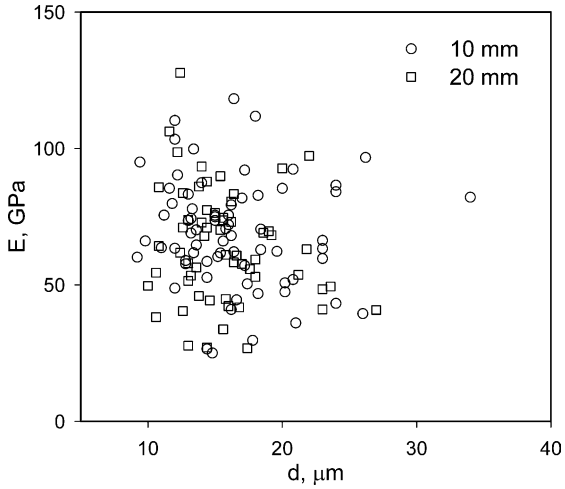

Fig. 6. Flax fibre modulus as a function of fibre diameter.

the modulus and non-linear strain increment ε_n are provided in Table 1. In view of the pronounced scatter, these results are in rough agreement with the estimated modulus value of about 80 GPa based on UD composite tests [20,21] for ArcticFlax fibres produced by FinFlax.

Fibre modulus slightly decreases with diameter increase as noted in [10,14,21], but the effect is small and largely overshadowed by the scatter, Fig. 6.

3.2. Strength distribution

The experimental fibre strength distribution yielded by SFT tests is shown in Weibull coordinates in Fig. 7. The Weibull distribution

$$P(\sigma) = 1 - \exp\left[-\frac{l}{l_0}\left(\frac{\sigma}{\beta_\sigma}\right)^{\alpha_\sigma}\right] \tag{1}$$

parameters from SFT tests were determined by the maximum likelihood method (MLM). In Eq. (1), α_σ is the shape parameter, β_σ is the scale parameter of the Weibull distribution, l designates fibre length and l_0 is the reference length. The parameter values at the gauge lengths tested are summarized in Table 2 (here in Eq. (1) and below the reference length is chosen as $l_0 = 1$ mm). It is seen that the two-parameter Weibull distribution approximates the experimental data at each of the gauge lengths reasonably well. Deviations from Weibull distribution are mostly confined to the weakest fibres and can be tentatively related to the damage done to the fibres in the specimen preparation process.

The dependence of the average fibre strength on the gauge length is plotted in Fig. 8 in logarithmic scale. The error bars correspond to the average strength standard deviation estimated as $s_\sigma/\sqrt{m}$, where s_σ and m are standard deviation of the fibre strength and the number of tests at the corresponding gauge length. It follows from Eq. (1) that the average strength is a power function of gauge length

$$\langle\sigma\rangle = \beta_\sigma (l/l_0)^{-1/\alpha_\sigma}\Gamma(1 + 1/\alpha_\sigma). \tag{2}$$

By approximating the data with Eq. (2) as shown in Fig. 8, estimates of the Weibull distribution parameters $\alpha_\sigma = 5.2$ and $\beta_\sigma = 1430$ MPa are obtained. The Weibull shape parameter derived applying Eq. (2) is considerably higher than that obtained from SFT at a fixed length and amounting to ~2.9 for the gauge length interval considered. This discrepancy in parameter values characterizing the fibre strength scatter at a fixed gauge length and the average strength dependence on the fibre length suggests that the modified Weibull distribution [22,23]

$$P(\sigma) = 1 - \exp\left(-\left(\frac{l}{l_0}\right)^{\gamma_\sigma}\left[\frac{\sigma}{\beta_\sigma}\right]^{\alpha_\sigma}\right) \tag{3}$$

is preferable to (1) for the flax fibres considered. The distribution (3) reconciles the mismatch of the fibre strength scatter at a fixed gauge length (characterized by α_σ) and the average strength dependence on the fibre length (governed by the exponent, $\gamma_\sigma/\alpha_\sigma$)

Table 1
Flax fibre deformation characteristics

Fibre length, mm	Average modulus $\langle E\rangle$, GPa	Standard deviation s_E, GPa	Average non-linear strain increment $\langle\varepsilon_n\rangle$, %	Standard deviation $s_{\varepsilon n}$, %
10	69	20	0.32	0.42
20	64	21	0.41	0.49

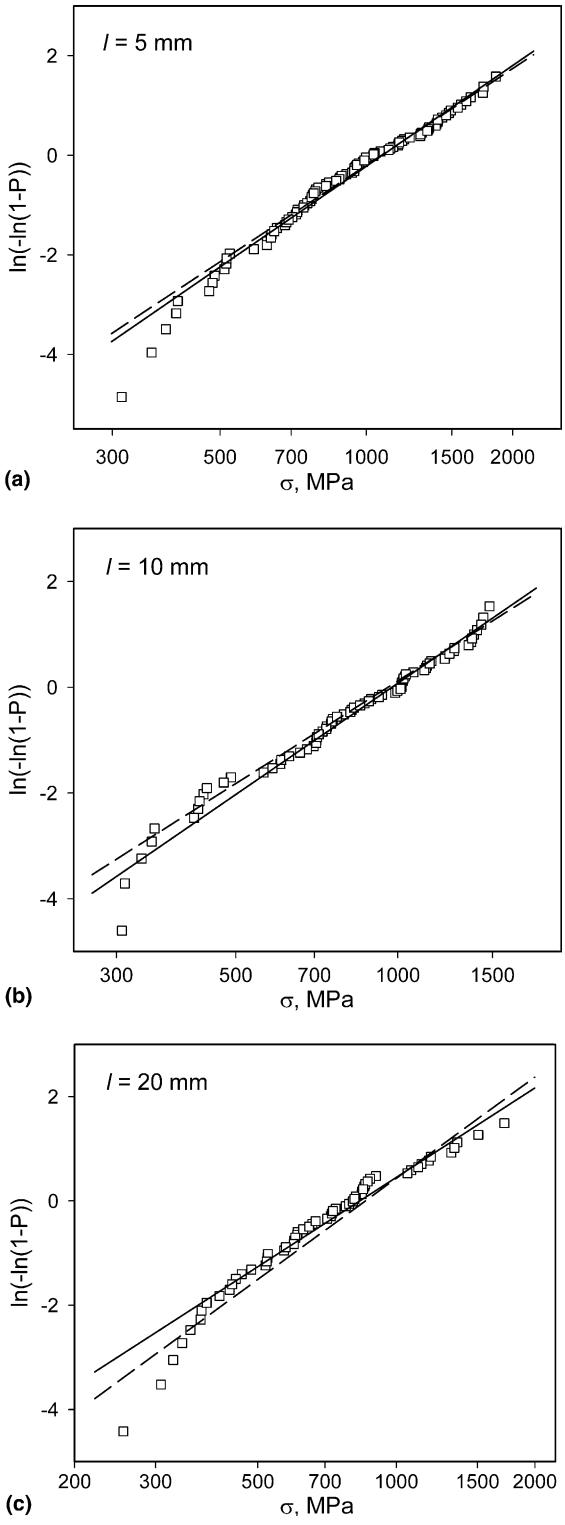

Fig. 7. Strength distribution of flax fibres at 5 (a), 10 (b), and 20 mm (c) gauge length. Solid lines – MLM approximation by two-parameter Weibull distribution equation (1), dashed lines – by modified Weibull distribution equation (3).

$$\langle\sigma\rangle = \beta_\sigma (l/l_0)^{-\gamma_\sigma/\alpha_\sigma} \Gamma(1 + 1/\alpha_\sigma). \tag{4}$$

It is suggested in [23,24,17] that the distribution (3) reflects the fibre-to-fibre strength parameter variation in a batch of fibres, each of which has the Weibull two-parameter strength distribution (1). The parameters of the distribution (3) determined by MLM from strength data in 5–20 mm gauge length interval are as follows: $\gamma_\sigma = 0.46$, $\alpha_\sigma = 2.8$, $\beta_\sigma = 1400$ MPa. The slope and location of the corresponding plots in Weibull coordinates, Fig. 7, are in good agreement with the SFT test data. Consequently, the modified Weibull distribution adequately describes both gauge length dependence of strength and the strength distribution at a fixed gauge length for the flax fibres considered.

Both axial stiffness and strength of flax fibres is imparted by the cellulose microfibrils, therefore it appears plausible that these quantities are correlated. Fig. 9 shows that a weak correlation is indeed present.

3.3. Failure strain distribution

Failure strain distributions were determined only for 10 and 20 mm flax fibres. The corresponding Weibull plots are given in Fig. 10. The parameter values of the two-parameter Weibull distribution for failure strain

$$P(\varepsilon) = 1 - \exp\left[-\frac{l}{l_0}\left(\frac{\varepsilon}{\beta_\varepsilon}\right)^{\alpha_\varepsilon}\right] \tag{5}$$

obtained by MLM are provided in Table 3.

For linear elastic fibres with negligible modulus scatter, the relation between failure strain and strength distributions is trivial – both share the same shape parameter $\alpha_\sigma = \alpha_\varepsilon$, and the scale parameter of the strength distribution is given by the product of fibre modulus and the corresponding strain distribution parameter, $\beta_\sigma = E\beta_\varepsilon$. Flax fibre stress–strain curve obtained by SFT typically possesses an initial non-linear zone as shown schematically in Fig. 4. Hence, flax fibre strength is related to its modulus, failure strain, and the non-linear strain increment, ε_n, as follows:

$$\sigma = E(\varepsilon - \varepsilon_n). \tag{6}$$

Note that all the fibre parameters entering Eq. (6) vary considerably between fibres. However, both failure strain and non-linear strain increment are virtually uncorrelated with the fibre modulus. Therefore, Eq. (6) remains valid also for average values of the parameters:

$$\langle\sigma\rangle = \langle E\rangle(\langle\varepsilon\rangle - \langle\varepsilon_n\rangle). \tag{7}$$

Thus Eq. (7) relates mean failure strain and fibre strength; accounting for mean stress expression Eq. (4), failure strain as a function of fibre length is given by

$$\langle\varepsilon\rangle = \beta_\sigma (l/l_0)^{-\gamma_\sigma/\alpha_\sigma} \Gamma(1 + 1/\alpha_\sigma)/\langle E\rangle + \langle\varepsilon_n\rangle. \tag{8}$$

The prediction by Eq. (8) complies with SFT test data, Fig. 11.

Table 2
Weibull distribution parameters of flax fibre strength obtained by SFT tests

Data reduction method	Gauge length, mm	Number of specimens	Shape parameter α_σ	Scale parameter β_σ, MPa
MLM	5	90	2.9	1870
	10	70	3.0	2080
	20	58	2.5	2800
Eq. (2)	5, 10, 20	–	5.2	1430

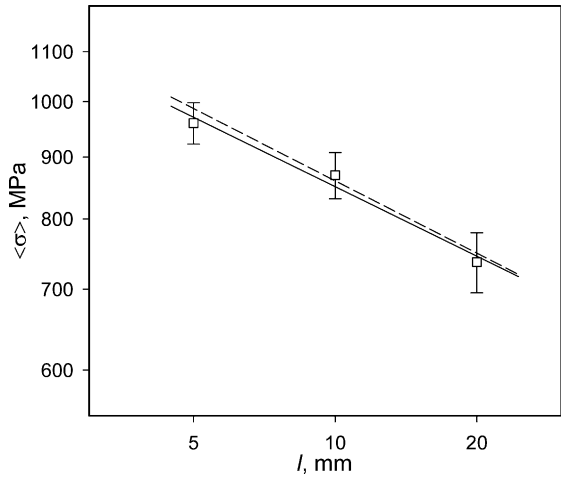

Fig. 8. Average fibre strength as a function of gauge length obtained by SFT tests. Solid line – approximation by Eq. (2), dashed line – prediction by SFF tests, Eq. (17).

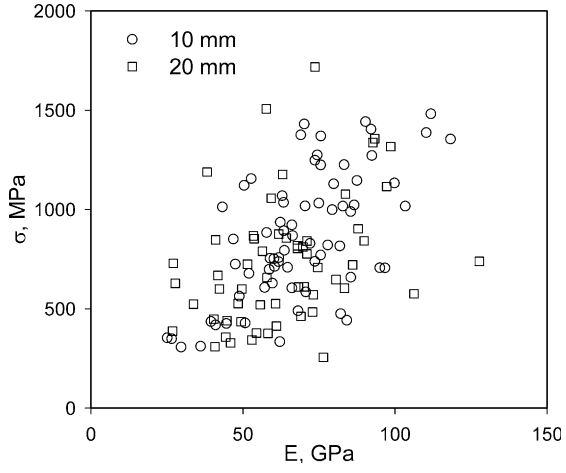

Fig. 9. Flax fibre strength as a function of fibre modulus.

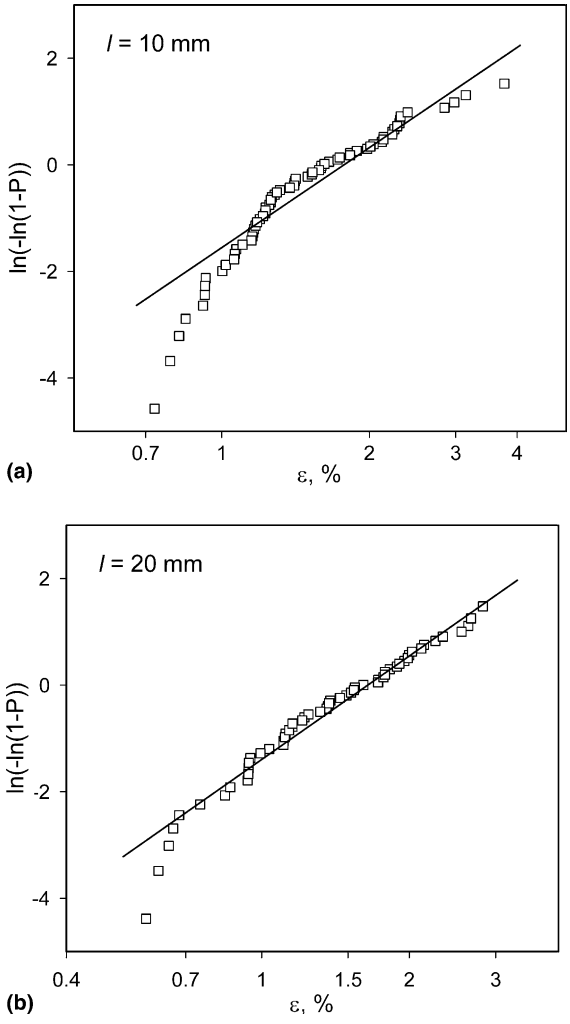

Fig. 10. Failure strain distribution of flax fibres at 10 (a) and 20 mm (b) gauge length. Solid lines – MLM approximation by two-parameter Weibull distribution equation (5).

Table 3
Weibull distribution parameters for failure strain of flax fibres

Test method	Gauge length, mm	Number of specimens	Shape parameter α_ε	Scale parameter β_ε, %
SFT	10	68	2.7	4.15
	20	56	2.8	4.79
SFF	~24	21	6.9	2.42

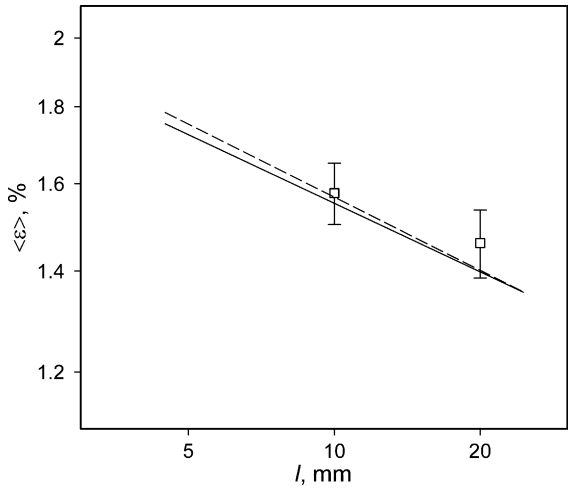

Fig. 11. Average failure strain as a function of gauge length obtained by SFT tests. Solid line – Eq. (8), dashed line – Eq. (16) based on SFF results.

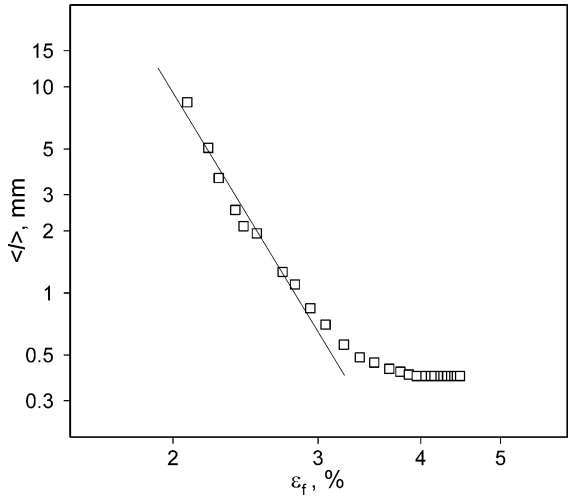

Fig. 12. Typical fibre fragmentation diagram showing the dependence of average fragment length on fibre strain and the approximation of the initial part of the diagram employed for Weibull parameter evaluation.

4. SFF tests

4.1. Analysis of fragmentation data

During the initial fragmentation stage when fibre break interaction is negligible the average fragment length, $\langle l\rangle$, of a fibre with Weibull failure strain distribution (5) is given by Eq. (9).

$$\langle l\rangle = l_0\left[\frac{\varepsilon_f}{\beta_\varepsilon}\right]^{-\alpha_\varepsilon}, \tag{9}$$

where ε_f is the fibre strain, $\varepsilon_f = \varepsilon_a + \varepsilon_r$, composed of the mechanical strain applied to the SFC, ε_a, and residual fibre strain, ε_r. A typical fragmentation diagram of elementary flax fibre is plotted in Fig. 12. The presence of a pronounced initial fragmentation stage with power-law dependence of average fragment length on fibre strain in agreement with Eq. (9) corroborates the applicability of Weibull distribution (5) for failure strain of individual fibres.

We estimated the residual fibre strain using fibre failure strain data obtained by SFT tests at a fixed gauge length so that the average fibre failure strain at the given gauge length derived from SFF tests is equal to the value obtained from SFT. The following iterative procedure was applied. An initial value for ε_r was assigned, and the Weibull distribution parameters for each SFC specimen were determined approximating the initial linear part of the fragmentation diagram in double logarithmic coordinates by (the logarithm of) Eq. (9) as shown in Fig. 12. Then the average failure strain for each SFF-tested fibre at a length l^*, $\varepsilon_i(l^*)$, was estimated using the obtained Weibull parameters as $\langle\varepsilon_i(l^*)\rangle = \beta_i(l^*/l_0)^{-1/\alpha_i}\Gamma(1+1/\alpha_i)$. The calculated failure strain values for SFF-tested fibres were averaged producing the fragmentation test estimate for average fibre failure strain at gauge length l^*, $\langle\varepsilon(l^*)\rangle = \frac{1}{n}\sum_{i=1}^{n}\langle\varepsilon_i(l^*)\rangle$, where n is the number of SFC tested. The obtained $\langle\varepsilon(l^*)\rangle$ value is compared with average fibre failure strain determined by SFT tests at the given gauge length, and the residual strain estimate adjusted accordingly. Such iterations are repeated until ε_r value at which $\langle\varepsilon(l^*)\rangle$ is equal to the average failure strain yielded by SFT test is found. Using average fibre failure strain at $l^* = 10$ mm gauge length as a benchmark, the residual strain was found to be $\varepsilon_r = -0.41\%$ in the case of VE matrix and $\varepsilon_r = -0.31\%$ for UP matrix.

Failure strain distribution (5) parameters obtained by SFF tests vary considerably between fibres as the Weibull plots for the parameters reveal, Fig. 13. The average values of the parameters are given in Table 3. The coefficient of variation for shape parameter, k_α, amounts to 0.30 and for scale parameter, k_β, to 0.13. It is interesting to note that a roughly comparable variability of Weibull distribution parameters was also obtained by SFF tests of *E*-glass fibres [17], namely $k_\alpha = 0.27$ and $k_\beta = 0.10$.

4.2. Modified Weibull distribution of fibre failure strain

It has been shown by numerical simulation [24] that the batch strength distribution of fibres, each of which has Weibull strength distribution (1) with the same shape parameter but randomly varying scale parameter (the latter also being Weibull-distributed), closely approximates the modified Weibull distribution (3). Flax SFF tests suggest that failure strain of individual fibres has Weibull distribution (5), and the variability of the scale parameter also agrees with Weibull distribution as revealed by the linearity of the corresponding Weibull plot, Fig. 13(b). However, the scatter of the Weibull shape parameter values is not negligible, Fig. 13(a). Therefore the

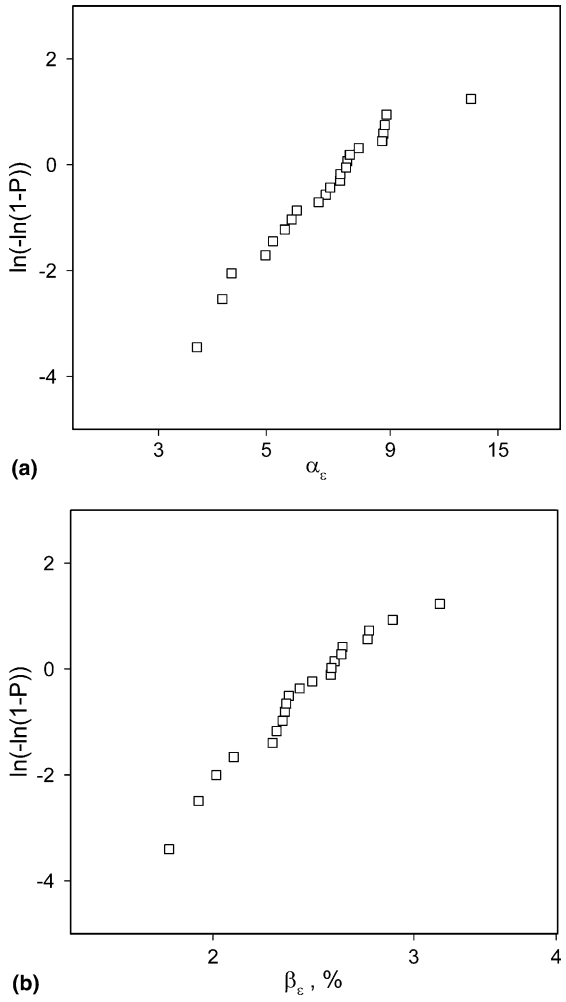

Fig. 13. Weibull plot of fibre failure strain distribution, Eq. (5), parameters α_ε (a) and β_ε (b) obtained by SFF tests.

approximate relations derived in [24] for parameters of the modified Weibull distribution are not applicable here.

Similar fibre-to-fibre variability of Weibull distribution parameters was also obtained in SFF tests of glass fibres, the strength of which complied with the modified Weibull distribution [17]. We apply the method proposed in [17] to estimate from SFF tests the parameters the modified Weibull distribution of failure strain

$$P(\varepsilon) = 1 - \exp\left(-\left(\frac{l}{l_0}\right)^{\gamma_\varepsilon}\left[\frac{\varepsilon}{\beta_\varepsilon}\right]^{\alpha_\varepsilon}\right). \tag{10}$$

Assuming that (i) the difference in Weibull parameter values obtained by SFF tests stems solely from the variation in fibre strength distribution parameters among fibres and (ii) the set of Weibull parameters determined by SFF tests fully describes the interfibre strength variability, we obtain [17]

$$\langle\varepsilon\rangle = \frac{1}{n}\sum_{i=1}^{n}\beta_i(l/l_0)^{-1/\alpha_i}\Gamma(1+1/\alpha_i), \tag{11}$$

$$s_\varepsilon = \left\{\frac{1}{n}\sum_{i=1}^{n}\beta_i^2\cdot(l/l_0)^{-2/\alpha_i}\Gamma(1+2/\alpha_i) - \left(\frac{1}{n}\sum_{i=1}^{n}\beta_i\cdot(l/l_0)^{-1/\alpha_i}\Gamma(1+1/\alpha_i)\right)^2\right\}^{1/2}, \tag{12}$$

where n is the number of fibres tested by SFF, and α_i, β_i are the Weibull parameters of the ith fibre. Further, equating the ratio of standard deviation and average failure strain provided by Eqs. (11) and (12) at $l = l_0$ to the coefficient of variation for limit strain according to Eq. (10), we obtain relation for the shape parameter of distribution (10)

$$\left.\frac{s_\varepsilon}{\langle\varepsilon\rangle}\right|_{l=l_0} = \sqrt{\frac{\Gamma(1+2/\alpha_\varepsilon)}{\Gamma(1+1/\alpha_\varepsilon)^2} - 1}. \tag{13}$$

Equating average strength and its derivative with respect to fibre length based on Eq. (11) and on distribution (10) result in

$$\langle\varepsilon\rangle|_{l=l_0} = \beta_\varepsilon\Gamma(1+1/\alpha_\varepsilon), \tag{14}$$

$$\left.\frac{\mathrm{d}\langle\varepsilon\rangle}{\mathrm{d}l}\right|_{l=l_0} = -\frac{\gamma_\varepsilon}{l_0\alpha_\varepsilon}\beta_\varepsilon\Gamma(1+1/\alpha_\varepsilon). \tag{15}$$

Solving Eq. (13) for α_ε and determining β_ε and γ_ε from Eqs. (14) and (15) yields the numerical values for distribution (10) parameters based on SFF test results as follows: $\gamma_\varepsilon = 0.79$, $\alpha_\varepsilon = 4.97$, $\beta_\varepsilon = 2.5\%$. The average failure strain as a function of fibre length according to Eq. (10)

$$\langle\varepsilon\rangle = \beta_\varepsilon(l/l_0)^{-\gamma_\varepsilon/\alpha_\varepsilon}\Gamma(1+1/\alpha_\varepsilon) \tag{16}$$

is plotted in Fig. 11 by dashed line. It is seen that the length dependence for fibre failure strain yielded by Eq. (16) agrees reasonably well with the SFT experimental data, although failure strain variability at fixed fibre length is underestimated.

Combining Eqs. (7) and (16), we obtain for average fibre strength

$$\langle\sigma\rangle = \langle E\rangle(\beta_\varepsilon(l/l_0)^{-\gamma_\varepsilon/\alpha_\varepsilon}\Gamma(1+1/\alpha_\varepsilon) - \langle\varepsilon_\mathrm{n}\rangle). \tag{17}$$

The relation (17) is reproduced in Fig. 8 against SFT experimental data. It is seen that Eq. (17) based on SFF tests can rather accurately predict the length effect of fibre strength. Thus a limited number of SFF tests combined with SFT tests at a fixed gauge length can provide the experimental information necessary for characterizing the scatter of fibre failure strain and strength and the effect of fibre length on the mentioned parameters.

5. Conclusions

Elementary flax fibre strength and failure strain distributions at several gauge lengths are obtained by SFT

tests. Strength and failure strain possess the modified Weibull distribution (i.e., independent exponents characterize strength scatter at a fixed gauge length and the dependence of mean strength on fibre length). SFF tests reveal that fibre fragmentation process proceeds in agreement with the two-parameter Weibull distribution of failure strain, Eq. (5), but the distribution parameters for individual fibres exhibit a marked scatter. A limited number of SFF tests combined with SFT tests at a fixed gauge length provide the experimental information necessary for characterizing both the scatter of fibre failure strain and strength at a fixed gauge length and the effect of fibre length on the mentioned parameters.

Acknowledgements

Undergraduate students Henrik Lindberg, Borsini Serena, Isidori Tatiana and graduate student Philippe Lingois were involved in this work.

This study is partially financed by the Swedish Royal Academy of Sciences.

Part of this study has been carried out with financial support from the Commission of the European Communities granted to the GROWTH Project GRD1-1999-10951 "ECOFINA". The study does not necessarily reflect the views of the European Commission.

Flax fibres for this study were supplied by partner in ECOFINA project, FINFLAX. Fibre surface treatment was performed by partner in ECOFINA project, University of Basque Country.

Appendix A. Verification of the extended fibre SFF test method

The intended role of fibre extensions is to hold the fibre in place while the resin solidifies. Once the resin has cured, the perturbation of the fibre stress due to the presence of extensions is expected to extend only by a limited distance, so-called stress transfer length, from the fibre ends. This distance, a function of fibre and resin moduli and typically an order of magnitude larger than fibre diameter, is to be excluded from monitoring for fibre cracks during fragmentation test.

In order to illustrate the principal features of stress transfer, we performed linear elastic analysis of the SFC under thermomechanical loading by finite element code ANSYS. To simplify analysis, Plane83 2-D 8-node axisymmetric elements (10,000 elements in total) were used to model SFC geometry of coaxial fibre and extension embedded in a resin cylinder; schematic picture of the model and example of the mesh are shown in Fig. 14. Symmetry conditions are enforced along the top edge of the model and vertical (y) axis, which is the line of axial symmetry. The thermoelastic properties of the

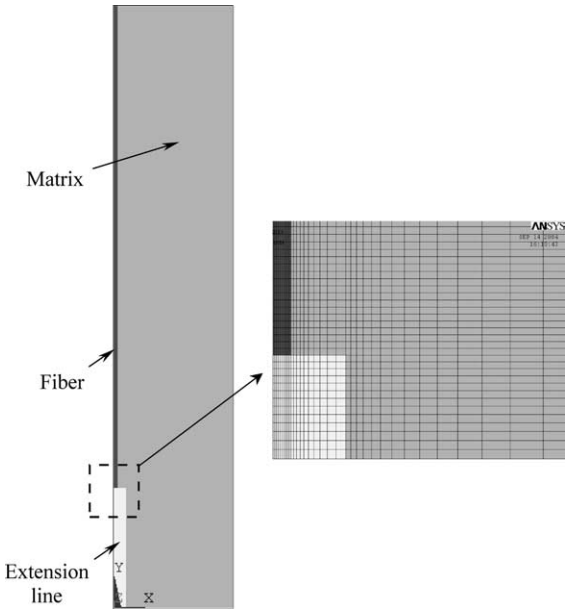

Fig. 14. Finite element model of the extended fibre SFC.

constituents were chosen as for glass fibre and VE matrix: fibre modulus $E_f = 74$ GPa, Poisson's ratio $\nu_f = 0.22$, coefficient of thermal expansion $CTE_f = 5 \times 10^{-6}$ 1 / °C; matrix modulus $E_m = 3$ GPa, Poisson's ratio $\nu_m = 0.35$, coefficient of thermal expansion $CTE_m = 6 \times 10^{-5}$ 1 / °C. The radius of the extension is taken four times larger than fibre radius, r_f, and that of the matrix cylinder is $40r_f$; the length of the extension line is $40r_f$, the fibre length is $160r_f$. The stress state in the SFC was calculated for thermal and for mechanical loading separately. The thermal loading is due to the temperature drop from a stress-free post-cure temperature to room temperature. The mechanical loading is accomplished by applying a uniform y -direction displacement to the bottom (i.e., $y = 0$) line of the model corresponding to the nominal applied strain of 1%. The calculated axial strain at the symmetry axis of the model ($x = 0$) in the extension and the fibre is shown in Fig. 15 as a function of the relative distance form the bottom edge of the model ($y = 0$). It is seen that the perturbation zone of the fibre strain extends for a distance of about $50r_f$ from the fibre/extension joint for the range of extension mechanical characteristics studied. (Note that the slight dependence of the calculated far-field fibre strain under mechanical load on the extension modulus, Fig. 15(b), is due to the rather limited cross-section area of the resin in the model as compared to the actual dimensions of the SFC's tested, Fig. 3).

In order to verify the applicability of the modified SFF test method, we performed a limited number of extended-fibre SFF tests for an E-glass fibre previously tested by the ordinary SFF method involving long fibres as reported in [17]. Short glass fibres of ca. 26 mm length were cut from continuous filaments separated from the glass fibre bundle. The fibre extensions

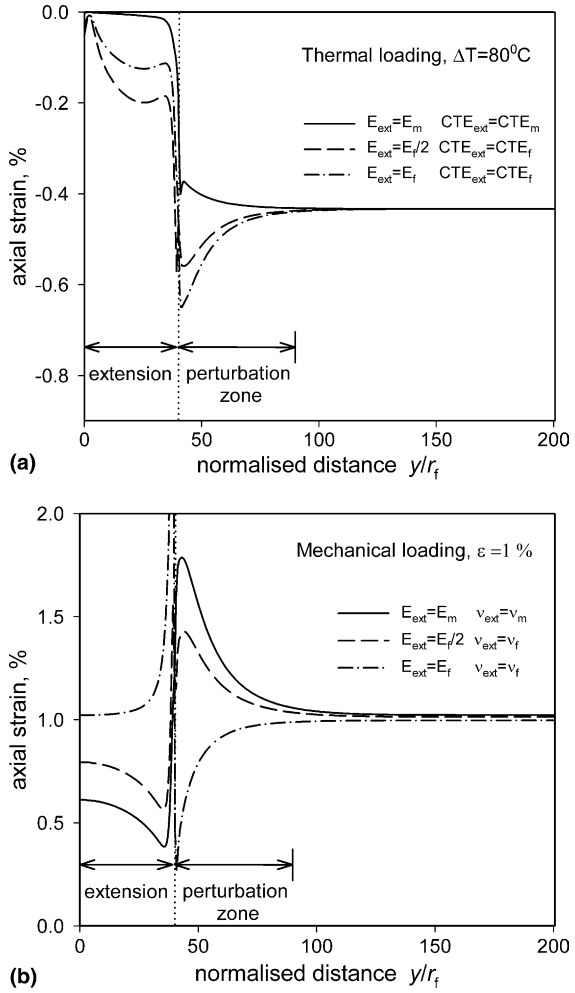

Fig. 15. Axial strain distribution in the extension and the fibre under thermal (a) and mechanical (b) loading. Dotted line shows the position of extension/fibre joint.

were attached and SFC specimens prepared following the routine described in Section 2.3.1; VE matrix was used. Fragmentation testing and data analysis was carried out in exactly the same way as described in [17] for long-fibre SFCs. The average values of the Weibull shape and scale parameters, based on four SFF tests, amounted to 8.0 (1) and 3150 (120) MPa respectively (here and below the number in brackets is the standard deviation of the corresponding average value). Twelve long-fibre SFF tests yielded the average shape parameter of 8.6 (.7) and scale parameter 3090 (90) MPa [17]. It is seen that the fibre strength distribution parameters obtained by the modified SFF test agree within experimental scatter with those obtained by the ordinary SFF procedure.

References

[1] Lilholt H, Lawther JM. Natural organic fibres. In: Kelly A, Zweben C, editors. Comprehensive composite materials, vol. 1. New York: Pergamon Press; 2000.

[2] Bledzki AK, Gassan J. Composites reinforced with cellulose based fibres. Progr Polym Sci 1999;24:221–74.

[3] Joshi SV, Drzal LT, Mohanty AK, Arora S. Are natural fiber composites environmentally superior to glass fiber reinforced composites?. Composites: Part A 2004;35:371–6.

[4] Magurno A. Vegetable fibres in automotive interior components. Die Angew Makromol Chem 1999;272:99–107.

[5] de Bruijn JCM. Natural fibre mat thermoplastic products from a processor's point of view. Appl Compos Mater 2000;7: 415–20.

[6] Davies GC, Bruce DM. Effect of environmental relative humidity and damage on the tensile properties of flax and nettle fibers. Text Res J 1998;68:623–9.

[7] Van de Velde K, Baetens E. Thermal and mechanical properties of flax fibres as potential composite reinforcement. Macromol Mater Eng 2001;286:342–9.

[8] Bos HL, van den Oever MJA, Peters OCJJ. Tensile and compressive properties of flax fibres for natural fibre reinforced composites. J Mater Sci 2002;37:1683–92.

[9] Van de Weyenberg I, Ivens J, Verpoest I. Parametric study of the relationship between the fibre and the composite properties of flax fibre reinforced epoxy. In: Proceedings of ECCM9, Brighton; June 2000.

[10] Joffe R, Andersons J, Wallström L. Strength and adhesion characteristics of elementary flax fibers with different surface treatments. Composites: Part A 2003;34:603–12.

[11] Van den Oever MJA, Bos HL. Critical fibre length and apparent interfacial shear strength of single flax fibre polypropylene composites. Adv Compos Lett 1998;7:81–5.

[12] Zafeiropoulos NE, Baillie CA, Matthews FL. A study of transcrystallinity and its effect on the interface in flax fibre reinforced composite materials. Composites: Part A 2001;32:525–43.

[13] Zafeiropoulos NE, Baillie CA, Hodgkinson JM. Engineering and characterisation of the interface in flax fibre/polypropylene composite materials. Part II. The effect of surface treatments on the interface. Composites: Part A 2002;33:1185–90.

[14] Baley C. Analysis of the flax fibres tensile behaviour and analysis of the tensile stiffness increase. Composites: Part A 2002;33:939–48.

[15] Drzal LT, Herrera-Franco PJ, Ho H. Fibre–matrix interface tests. In: Kelly A, Zweben C, editors. Comprehensive composite materials, vol. 5. New York: Pergamon Press; 2000.

[16] Andersons J, Joffe R, Hojo M, Ochiai S. Fibre fragment distribution in a single-fibre composite tension test. Composites: Part B 2001;32:323–32.

[17] Andersons J, Joffe R, Hojo M, Ochiai S. Glass fibre strength distribution determined by common experimental methods. Compos Sci Technol 2002;62:131–45.

[18] Eichhorn SJ, Young RJ. Composite micromechanics of hemp? bres and epoxy resin microdroplets. Compos Sci Technol 2004;64:767–72.

[19] Hornsby PR, Hinrichsen E, Tarverdi K. Preparation and properties of polypropylene composites reinforced with wheat and flax straw fibres. Part I Fibre characterization. J Mater Sci 1997;32:443–4.

[20] Oksman K. Mechanical properties of resin transfer molded natural fiber composites. In: The fifth international conference on woodfiber–plastic composites, 1999. p. 97–103.

[21] Oksman K. High quality flax fibre composites manufactured by the resin transfer moulding process. J Reinf Plast Compos 2001;20:621–7.

[22] Gutans JA, Tamuzh VP. Scale effect of the Weibull distribution of fibre strength. Mech Compos Mater 1984(6):1107–9 [in Russian].

[23] Watson AS, Smith RL. An examination of statistical theories for fibrous materials in the light of experimental data. J Mater Sci 1985;20:3260–70.

[24] Curtin WA. Tensile strength of fiber-reinforced composites: III. Beyond the traditional Weibull model for fiber strengths. J Compos Mater 2000;34(15):1301–32.